Deformation Behavior of HCP Ti-Al Alloy Single Crystals

J.C. WILLIAMS, R.G. BAGGERLY, and N.E. PATON

Single crystals of Ti-Al alloys containing 1.4, 2.9, 5, and 6.6 pct Al (by weight) were oriented for $\langle \mathbf{a} \rangle$ slip on either basal or prism planes or loaded parallel along the *c*-axis to enforce a nonbasal deformation mode. Most of the tests were conducted in compression and at temperatures between 77 and 1000 K. Trace analysis of prepolished surfaces enabled identification of the twin or slip systems primarily responsible for deformation. Increasing the deformation temperature, Al content, or both, acted to inhibit secondary twin and slip systems, thereby increasing the tendency toward strain accommodation by a single slip system having the highest resolved stress. In the crystals oriented for basal slip, transitions from twinning to multiple slip and, finally, to basal slip occurred with increasing temperature in the lower-Al-content alloys, whereas for Ti-6.6 pct Al, only basal slip was observed at all temperatures tested. A comparison of the critically resolved shear stress (CRSS) values for basal and prism slip as a function of Al content shows that prism slip is favored at room temperature in pure Ti, but the stress to activate these two systems becomes essentially equal in the Ti-6.6 pct Al crystals over a wide range of temperatures.

Compression tests on crystals oriented so that the load was applied parallel to the *c*-axis showed extensive twinning in lower Al concentrations and $\langle \mathbf{c} + \mathbf{a} \rangle$ slip at higher Al concentrations, with a mixture of $\langle \mathbf{c} + \mathbf{a} \rangle$ slip and twinning at intermediate compositions. A few tests also were conducted in tension, with the load applied parallel to the *c*-axis. In these cases, twinning was observed, and the resolved shear for plastic deformation by twinning was much lower that that for $\langle \mathbf{c} + \mathbf{a} \rangle$ slip observed in compression loading.

I. INTRODUCTION

THE solid-solution strengthening and deformation behavior of the hexagonal α phase in Ti alloys plays a major role in determining the properties of most of the technologically significant Ti alloys in use today. The details of α-phase deformation control the strength of α and $\alpha + \beta$ alloys and are also important in deformation processing. The rolling texture (preferred orientation) observed in a commercially produced, hot-rolled sheet is controlled by the ratios of plastic strain accommodated by the various slip and twinning systems of the hexagonal α phase. For certain applications, controlled texture of a specified type can result in an ~30 pct increase in the Young's modulus, or an ~40 pct increase in yield strength under balanced biaxial tension.[1] A preferred orientation also can exert a marked influence on stress-corrosion susceptibility.[2]

The deformation behavior of hexagonal α-titanium has been extensively studied.[3–8] These studies have shown that many complex twinning and slip modes are responsible for the ductility exhibited by titanium. These complexities are due, in large part, to the crystallographic nature of the α phase, which has the hcp structure at temperatures up to at least 1150 K, depending on Al concentration. The degree of complexity is merely increased by the addition of alloying elements such as Al. The effect of Al is especially important, because it is a major addition in commercial α and $\alpha + \beta$ titanium alloys.

Several investigations have clearly established that the principal deformation mechanism in pure titanium is first-order prismatic slip, $\{10\bar{1}0\}\langle 11\bar{2}0\rangle$. Studies have been reported concerning details of the effect of oxygen additions on this deformation mode, but only a limited amount of work has been published on the effect of Al, with the studies being confined to a limited range of compositions and temperatures, partly due to the difficulty of growing large Ti-Al single crystals. Cass,[7] in a study of Ti-3 pct Al and Ti-7 pct Al crystals, showed that Al appears to increase the propensity for $\langle \mathbf{c} + \mathbf{a} \rangle$ slip, but he did not attempt to determine the effect of Al on the critically resolved shear stress (CRSS) for the various slip systems.

Sakai and Fine[8] have investigated the effect of up to 3.1 pct Al on the CRSS for prism slip from 77 to 600 K. They showed that Al additions to titanium reduce the CRSS for prism slip up to about 0.6 pct Al, but this is followed by solution hardening up to the 3.1 pct Al composition. They attributed the solid-solution softening to scavenging of interstitials.

There are six possible slip systems in the α phase.[9] There are two important slip vectors in the deformation processes: $\langle \mathbf{a} \rangle$ and $\langle \mathbf{c} + \mathbf{a} \rangle$. Of these, $\langle \mathbf{a} \rangle$ slip is most commonly observed.[6] The Burgers vector for $\langle \mathbf{a} \rangle$ slip can be described in the four-index (Miller–Bravais) notation by $1/3\langle 11\bar{2}0\rangle$, and the $\langle \mathbf{c} + \mathbf{a} \rangle$ Burgers vector is described by $1/3\langle 11\bar{2}3\rangle$. There are also a number of twinning modes which can operate in the α phase.[10] The presence of oxygen and/or Al is effective in suppressing twinning; thus, in the absence of twinning, $\langle \mathbf{c} + \mathbf{a} \rangle$ slip[11] is required to allow the grains in

J.C. WILLIAMS, Dean of Engineering and Honda Professor, is with The Ohio State University, Columbus, OH 43210. Contact e-mail: williams.1726@osu.edu R.G. BAGGERLY is a Metallurgical Consultant, Anacortes, WA 98221. N.E. PATON, retired Vice President, Howmet Corporation, is Metallurgical Consultant, Thousand Oaks, CA 91361.

This article is based on a presentation made in the symposium entitled "Defect Properties and Mechanical Behavior of HCP Metals and Alloys" at the TMS Annual Meeting, February 11–15, 2001, in New Orleans, Louisiana, under the auspices of the following ASM committees: Materials Science and Critical Technology Sector, Structural Materials Division, Electronic, Magnetic & Photonic Materials Division, Chemistry & Physics of Materials Committee, Joint Nuclear Materials Committee, and Titanium Committee.

a polycrystalline specimen to undergo an arbitrary shape change during plastic deformation. Moreover, in the absence of twinning, $\langle \mathbf{c} + \mathbf{a} \rangle$ slip is the only mode which permits a shape change that has a *c*-axis component. The ease or difficulty of operation of this slip mode directly influences the effectiveness of texture in altering the strength of a Ti alloy sheet.[1]

The present investigation was conducted to determine the effect of Al contents higher than those studied by Sakai and Fine[8] and to determine the effect of temperature on prism and basal slip from 77 to 1000 K. Al contents up to 6.6 pct were used, and this was high enough to permit the precipitation of some ordered Ti_3Al, α_2 phase after suitable aging treatments. Some aged crystals were tested to determine the effect of α_2 precipitates on the CRSS, since α_2 has been shown to precipitation harden Ti-Al polycrystals.[13,14]

Our approach was to study an individual deformation mode by orienting Ti-Al single crystals in order to maximize the resolved shear stress for a given slip system. These crystals were tested in compression at temperatures ranging from 77 K to near the α-β transus, or 1000 K. Using this approach, we were able to determine the CRSS for $\langle \mathbf{a} \rangle$ slip in crystals oriented for basal and prism slip. Similarly, we have determined the CRSS for nonbasal deformation modes in crystals oriented with the loading axis parallel to the *c*-axis. In these tests, twinning and $\langle \mathbf{c} + \mathbf{a} \rangle$ slip were observed, depending on test temperature, Al concentration, and purity.

II. EXPERIMENTAL PROCEDURE

Single crystals of Ti-Al alloys were grown in the form of cylindrical rods using the floating-molten-zone technique in an ion-pumped electron-beam melting furnace. The starting materials were electrolytic-grade El-60 titanium, supplied by Titanium Metals Corp. of America (Henderson, NV), and 99.999 pct Al, supplied by United Mineral Corporation (New York, NY). These materials were arc melted and swaged to 6.4-mm-diameter rods prior to electron-beam melting. Single crystals approximately 50-mm long could be routinely grown, having compositions of up to 6.6 wt pct Al. The compositions in wt pct used for this investigation were 1.4, 2.9, 5, and 6.6 pct Al.

Sections of the as-grown crystals were oriented using Laue X-ray diffraction methods. The crystals were then potted in epoxy, using a rectangular mold to maintain the correct crystal orientation, and subsequently sliced and polished. An anneal of 8 hours at 1125 K in a vacuum of 6.6×10^{-4} Pa followed the final electropolish, which was performed at 245 K using the same solution as that used for preparing transmission electron microscope foils.[15] Finished specimens were in the shape of right rectangular prisms of dimensions $0.6 \times 0.6 \times 1.2$ cm high (Figure 1(a)). These crystals, intended to deform by basal slip on the (0001)$[11\underline{2}0]$ system, were oriented for the loading axis 45 deg to the (0001) plane, to within ± 2 deg (Figure 1(b)). The two orthogonal faces, which were used for trace analysis, were parallel to the $(10\underline{1}0)$ and close to the $(11\underline{2}3)$ planes. The crystals oriented for prism slip were loaded along $[\underline{1}100]$, with the two faces used for trace analysis being (0001) and $\{11\underline{2}0\}$, as shown in Figure 1(c). The *c*-axis crystals were loaded along the [0001] and the two orthogonal faces, which were used for trace analysis were parallel to $\{10\underline{1}0\}$ and $\{11\underline{2}0\}$ planes (Figure 1(d)).

Compressive loading was accomplished with an Instron machine at a strain rate of 4×10^{-4} s^{-1}. Liquid nitrogen was used for the 77 K tests, dry ice and methanol were used for the 190 K tests, silicon oil was used for temperatures above room temperature to 600 K, and a vacuum furnace operating at less than 1.3×10^{-3} Pa was used for testing between 600 and 1000 K.

The surface features of the deformed crystals were examined with a scanning electron microscope, as well as a Zeiss light microscope equipped with polarizer and Nomarski interference lenses. Thin sections for transmission electron microscopy (TEM) observations parallel and normal to the slip planes were spark machined from the specimen and electrothinned using the standard Ti electrolyte.[15]

III. RESULTS

A. *Crystals Oriented for Basal Slip*

The effect of Al content and test temperature resulted in marked variations in deformation characteristics. Although specimens were optimally oriented for basal slip, the resolved stress on other slip and twinning systems was generally nonzero, and, frequently, the tendency was to deform by twinning in the low-Al-content crystals. The effect of increasing temperature was seen to suppress twinning and promote basal slip. The temperature dependence of the resolved shear stress for the onset of plastic deformation by basal slip is shown in Figure 2 for the compositions tested. Undulations in the resolved-shear-stress curves could be associated with transitions between deformation by twinning and by slip.

1. *Ti-6.6 pct Al*

The Ti-6.6 pct Al crystals deformed by the (0001)$\langle 11\underline{2}0 \rangle$ slip system for all temperatures tested. Observations of the slip-line structure showed that as the temperature increased, the slip character changed from fine planar slip to coarse planar slip, examples of which are shown in Figures 3(a) and (b). The slip was confined to well-defined planes which coincided with the basal plane, (0001). The Al content was high enough to permit α_2-phase precipitation on prolonged aging. For example, aging these crystals at 825 K for one week produced a very fine, uniform distribution of α_2 particles. An example of the α_2 size and distribution is shown in Figure 4(a). A mean α_2 particle size of 6 nm was determined using X-ray diffraction line-broadening techniques. Figure 3 showed that these precipitates have a significant effect on the slip character of the single crystals, producing coarse, well-defined slip bands in which the slip was more confined and the distances between slip bands greater. A coarse, planar slip band is shown in Figure 4(b), which is a dark-field micrograph showing that the α_2 precipitates have been effectively destroyed within the slip band by repeated shearing. A TEM study of these crystals also showed that the slip bands contained planar dislocation arrays, as shown in Figure 5. However, as the deformation temperature increased, there was a marked tendency for the aged crystals to exhibit cross slip onto prism planes. At the intersection of two or more cross-slip planes, regions resembling nuclei of recrystallized grains could be seen. To investigate the possibility of these regions being hydrides, the foil was heated to 625 K in a hot stage. This did not produce a noticeable change in the appearance of these

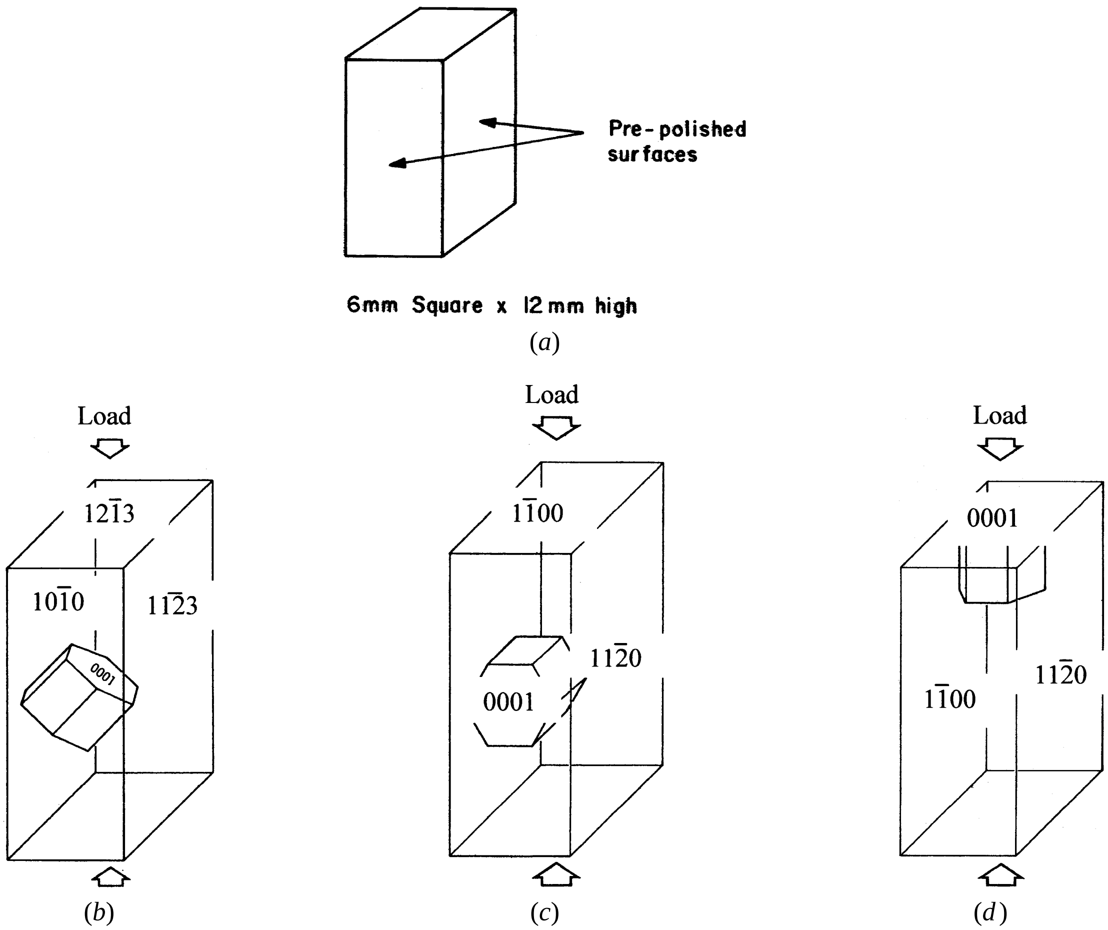

Fig. 1—Compression specimen geometry and orientation of crystals for basal, prism, and *c*-axis resolved shear stress measurements: (*a*) specimen geometry, (*b*) basal slip geometry, (*c*) prism slip geometry, and (*d*) *c*-axis specimen geometry.

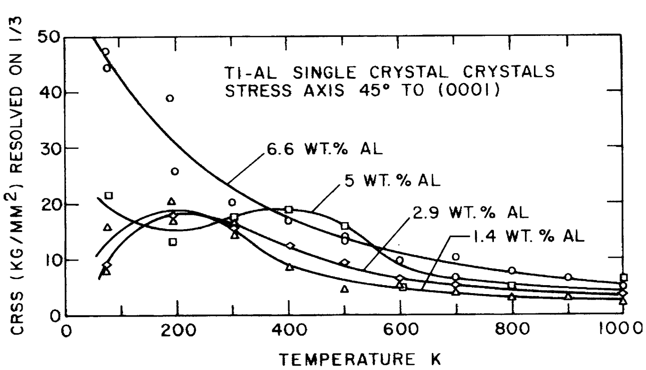

Fig. 2—Critical resolved shear stress for basal slip *vs T* for crystals with four Al concentrations.

nuclei, indicating that, in fact, they are not hydrides. Bright- and dark-field TEM micrographs corroborating this are shown in Figures 6(a) and (b), respectively.

Deformation at elevated temperatures generally did not produce the hexagonal networks of ⟨**a**⟩ dislocations which are commonly observed in polycrystalline titanium that has been hot worked.[16] The formation of these networks requires the presence of dislocations with all three ⟨**a**⟩-type Burgers vectors. Typically, in single crystals oriented for single or duplex slip, all three are not present and net formation would not be expected.

2. *Ti-5 pct Al*

The temperature dependence of the CRSS for basal slip in Ti-5 pct Al crystals (Figure 2) shows an initial increase, a secondary peak near 400 K, and then a decrease. This is in contrast to the monotonically decreasing curve for Ti-6.6 pct Al. The evidence suggests that these variations are a result of a transition in the deformation mechanisms for this alloy. At 77 and 190 K, deformation occurred primarily by twinning on $\{11\underline{2}1\}$ planes. The TEM micrographs (Figures 7(a) and (b)) show significant twinning, as well as considerable dislocation-slip activity within the twins, and accommodation slip in the matrix adjacent to the twins. The dislocations in the twins were of the ⟨**c** + **a**⟩ type, and accommodation dislocations in the matrix are also of this type.

At 300 K, there was a marked change in the deformation mode to predominantly basal slip, although some twinning persisted. Figures 8(a) and (b) show the large, local shear strains along the basal planes produced by slip on (0001). In Figure 8(b), the vertical traces, which are sheared by basal slip, conform to traces of very thin $\{11\underline{2}1\}$ twins. Although these twins obviously formed prior to slip on basal planes, the dominant deformation mode from a strain-accommodation standpoint was basal slip. A TEM micrograph (Figure 9) shows that the dislocation character associated with basal slip consists of long, straight, nearly pure screw dislocations and a considerable amount of debris (loops and

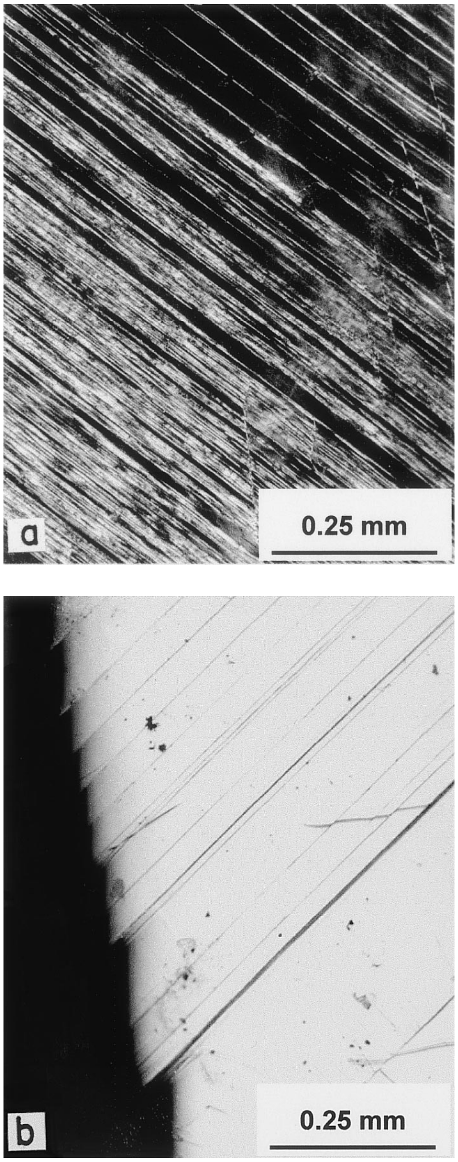

Fig. 3—Ti-6.6 pct Al crystal strained at 77 K: (*a*) solution treated at 1175 K; and (*b*) aged at 825 K for 1 week.

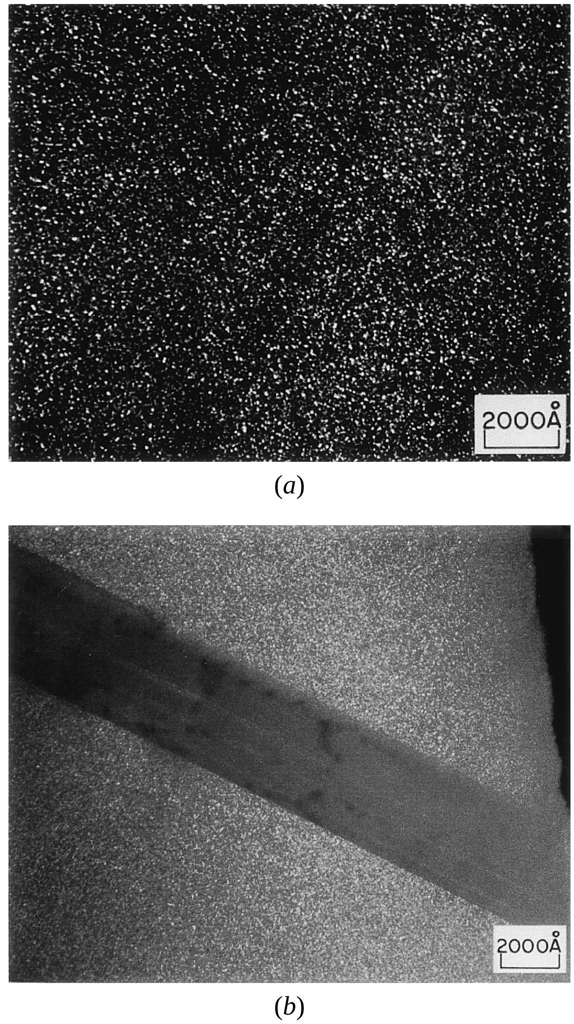

Fig. 4—Dark-field TEM photos taken with $\{10\bar{1}1\}$ α_2 reflection: (*a*) showing size and distribution of α_2 precipitates and (*b*) showing a slip band in which the α_2 precipitates have essentially been destroyed.

dipoles). With increasing temperature, there was a tendency for cross slip to occur, as can be seen from the slip lines in Figure 10. At higher temperatures, there was an increasing tendency to form hexagonal nets, indicating the presence of dislocation with all three $\langle \mathbf{a} \rangle$ vectors (Figure 11). These regions of hexagonal nets were, however, in the minority, and most areas of the foil showed dislocations with significant curvature and no nets. The cause of net formation is discussed elsewhere.[15]

3. *Ti-2.9 pct Al*

The deformation behavior of Ti-2.9 pct Al crystals varied considerably with temperature. Although twinning was evident at all temperatures tested, very planar basal slip did not occur until the test temperature exceeded 400 K. At 400 K, there was greater tendency for prism slip and $\{11\bar{2}1\}$ twinning, whereas at 500 K, basal slip and $\{11\bar{2}1\}$ twinning were the dominant deformation modes. With higher temperatures, twinning was further suppressed. In the resolved shear stress–temperature curves of Figure 2, the curve for Ti-2.9

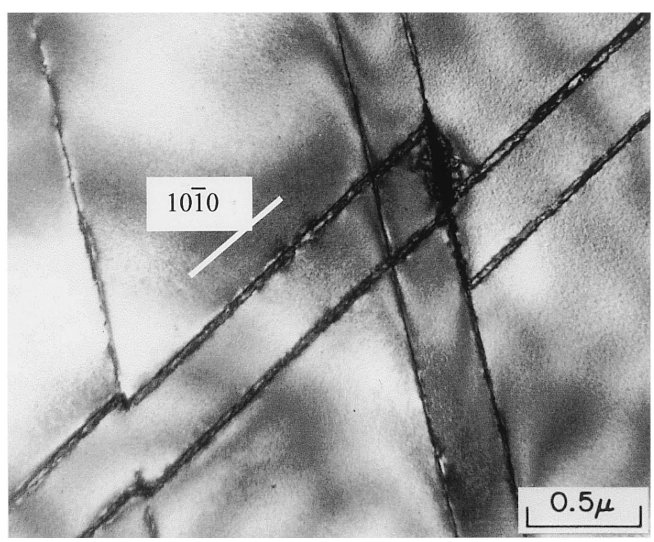

Fig. 5—Bright-field TEM micrographs showing prism slip bands that have been sheared by secondary prism slip; plane of foil (0001).

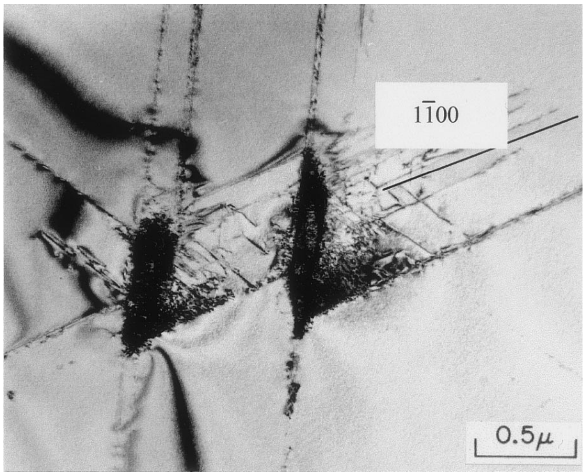

(*a*)

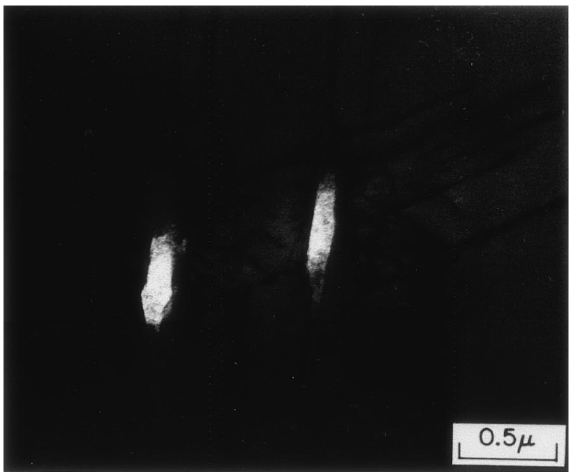

(*b*)

Fig. 6—Bright- and dark-field TEM pair showing recrystallized grain embryo at the intersection of two prism slip bands, plane of foil (0001): (*a*) bright field and (*b*) dark field.

pct Al increases from 77 K to a maximum at 200 K and then decreases with further temperature increase. Optical micrographs at 77 and 190 K show extensive twinning on $\{11\bar{2}1\}$ planes at 77 K (Figure 12(a)) and twinning plus basal-slip activity at 500 K (Figure 12(b)). The TEM micrographs and selected-area diffraction also permitted verification of this twin system. The TEM examination also showed pronounced $\langle \mathbf{c} + \mathbf{a} \rangle$ dislocation activity at the twin interfaces, similar to that shown in Figure 7(b). At 500 K, the basal-slip lines are very planar when viewed on a $\{11\bar{2}0\}$ face. Shear offsets in the basal-slip band suggested that basal slip occurred prior to twinning. The light micrographs showing these shears were used to make detailed measurements of the twinning shear for the $\{11\bar{2}1\}$ twins. The results agree with the earlier measurements of Reed–Hill on polycrystalline zirconium.[17] At 1000 K, the basal-slip lines became even better defined.

4. *Ti-1.4 pct Al*

The low-temperature deformation behavior consisted of extensive $\{11\bar{2}1\}$ twinning and dislocation slip on prism planes. Increasing the temperature led to decreased twinning and greater dislocation-slip activity, and at 300 K, prism slip

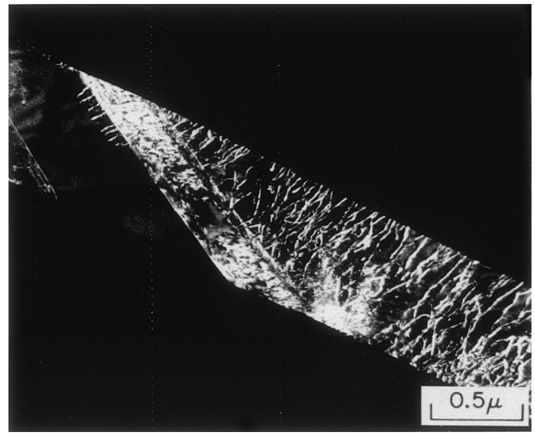

(*a*)

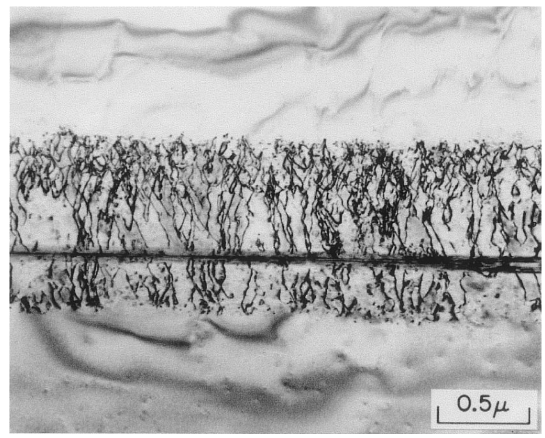

(*b*)

Fig. 7—TEM micrographs showing details of twin formation in Ti-5 pct Al: (*a*) dark field of twin showing internal slip, $\mathbf{g}_{0002\ \mathrm{twin}}$; and (*b*) bright field showing $\langle \mathbf{c} + \mathbf{a} \rangle$ accommodation slip in matrix; $\mathbf{g}_{0002}$.

dominated. As shown later, this is because the resolved shear stress for prism slip is much lower than for basal slip. Typical deformation structures are shown in Figures 13(a) through (d). As the deformation temperature further increased, so did the propensity for slip on (0001) and, at 1000 K, the slip lines became more planar. At this temperature, cross slip was fairly easy, and well defined basal-slip traces and cross-slip traces on $\{10\bar{1}1\}$ planes were apparent.

B. *Crystals Oriented For Prism Slip*

The addition of Al to titanium was found to have a disproportionate effect on the CRSS for prism slip, when compared to basal slip. The temperature dependence of the CRSS for $\langle \mathbf{a} \rangle$ slip on $\{10\bar{1}0\}$ prism planes is shown in Figure 14. Similar data for pure (iodide-grade) titanium have been included in this graph for purposes of comparison.[3,4] At 77 K, a small volume fraction of thin $\{10\bar{1}2\}$ twins were formed with $\langle \mathbf{c} + \mathbf{a} \rangle$ accommodation slip in the matrix, similar to that shown in Figure 15. At higher temperatures, only prism slip with an $\langle \mathbf{a} \rangle$ vector was observed. As the deformation temperature was increased, cross slip onto $\{10\bar{1}1\}$ planes became more prevalent. At 1000 K, dislocation arrangements consisting of straight screws, $\langle \mathbf{a} \rangle$ dislocations with numerous jogs, and debris in the form of small loops were

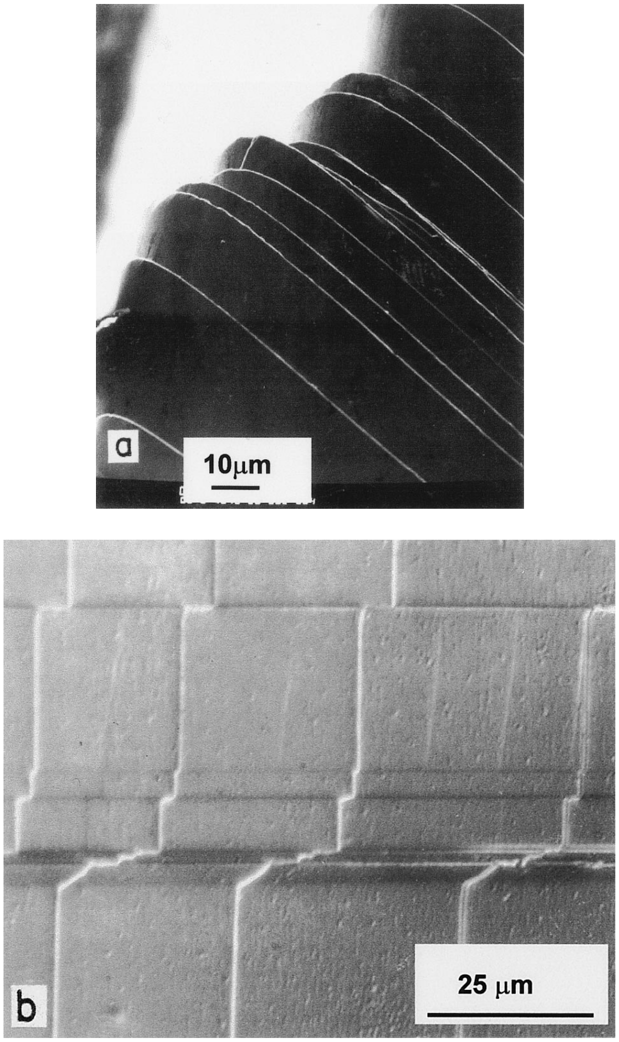

Fig. 8—SEM and light micrographs showing intense planar basal slip in Ti-5 pct Al: (*a*) SEM photo of corner of rectangular single-crystal prism showing slip offsets and (*b*) light micrograph showing intense basal slip bands that have sheared thin $\{11\bar{2}1\}$ twins.

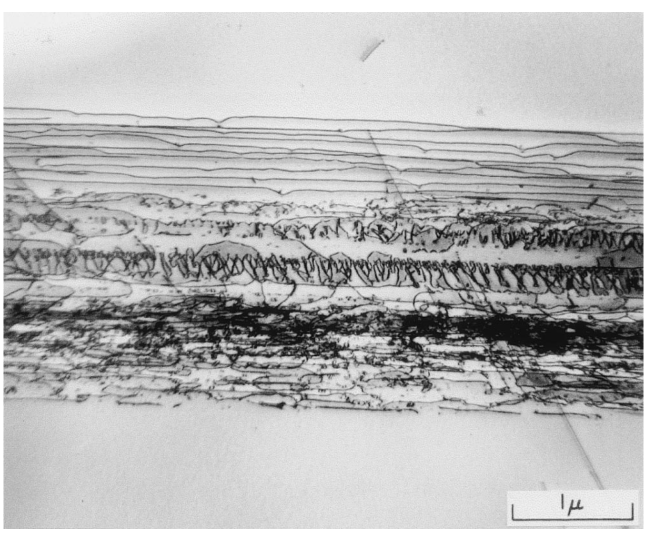

Fig. 9—Bright-field TEM micrograph of slip band in Ti-5 pct Al showing long, straight screw dislocation segments, extensive dipole formation, and dislocation debris.

Fig. 10—Light micrograph showing extensive cross slip from basal planes onto prism planes in Ti-5 pct Al deformed at 1000 K.

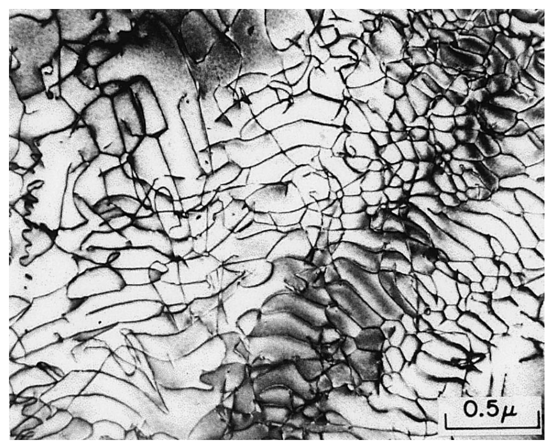

Fig. 11—Bright-field TEM micrograph showing early stages of hexagonal network formation Ti-5 pct Al deformed at 1000 K; image condition systematic multistrong $\mathbf{g}_{10\bar{1}1}$.

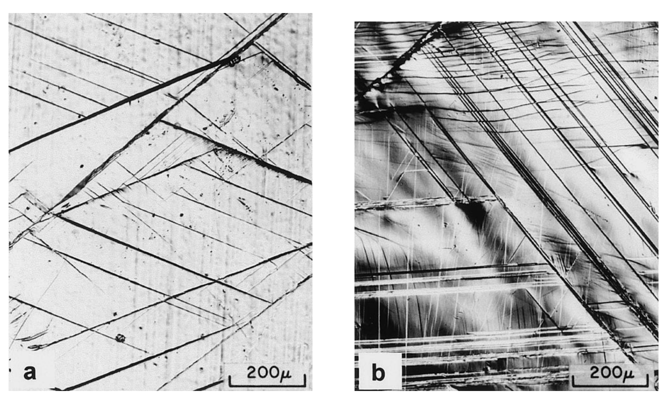

Fig. 12—Light micrographs showing deformation behavior of Ti-2.9 pct Al as a function of deformation temperature: (*a*) 77 K showing $\{11\bar{2}1\}$ twins and (*b*) 500 K showing $\{11\bar{2}1\}$ twins and basal slip.

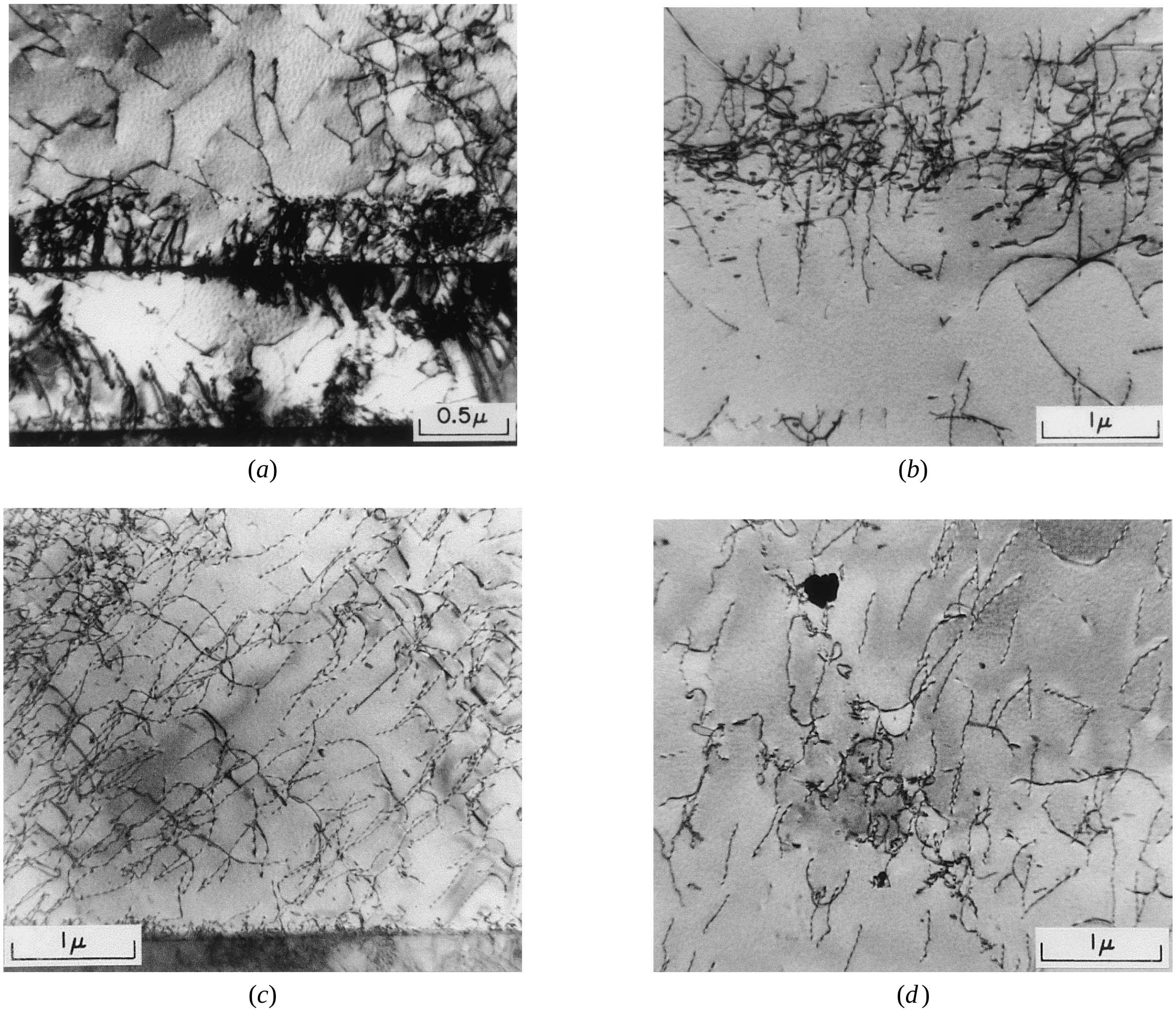

Fig. 13—Bright TEM micrographs showing changes in deformation behavior of Ti-1.4 pct Al basal orientation crystals as a function of temperature: image condition systematic multistrong $\mathbf{g}_{10\bar{1}1}$: (*a*) 77 K, (*b*) 300 K, (*c*) 500 K, and (*c*) 600 K.

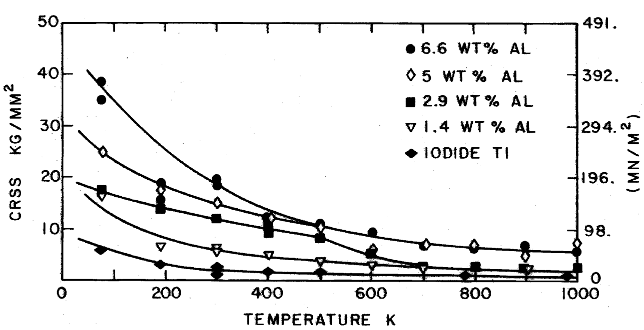

Fig. 14—Critical resolved shear stress for ⟨**a**⟩ slip on prism planes as a function of deformation temperature for four Al concentrations and for pure (iodide) Ti.

characteristic. The slip-plane traces observed on the surface were very planar at the lower test temperatures. With increasing deformation temperature, the propensity for cross slip increased, as evidenced by the tendency to form wavy slip bands similar to the case for basal slip. This behavior is shown by the micrographs of Figure 15 for Ti-5 wt pct Al at 77, 400, 600, and 1000 K.

A further effect of Al was to reduce the width of slip bands at a given test temperature. In contrast, increasing the deformation temperature leads to wider slip bands, with a reduced density of dislocations within the each band. The addition of Al results in a more planar distribution of dislocations, with a higher density of dislocations within the active slip bands. This is shown in Figure 16 for Ti-1.4 pct Al and Ti-6.6 pct Al crystals. Subgrain boundaries were always present in these crystals as substructure remaining from crystal growth. These boundaries were apparently relatively weak barriers to dislocation motion, as slip bands were observed to penetrate and displace the boundary, as shown in Figure 17. These boundaries are walls of ⟨**a**⟩-type dislocations, as best seen in Figure 17. These dislocations are most likely the source of the other ⟨**a**⟩-type dislocations that lead to hexagonal network formation (Figure 11) during high-temperature deformation of crystals that are nominally oriented for single slip. Large local offsets in these boundaries can be seen in Figure 17, which gives an indication of how highly localized the planar slip is.

In iodide titanium, deformation by $\{10\bar{1}2\}$ twinning contributes to the overall strain during loading.[3] The addition of 5 wt pct Al largely suppressed twinning when the crystals

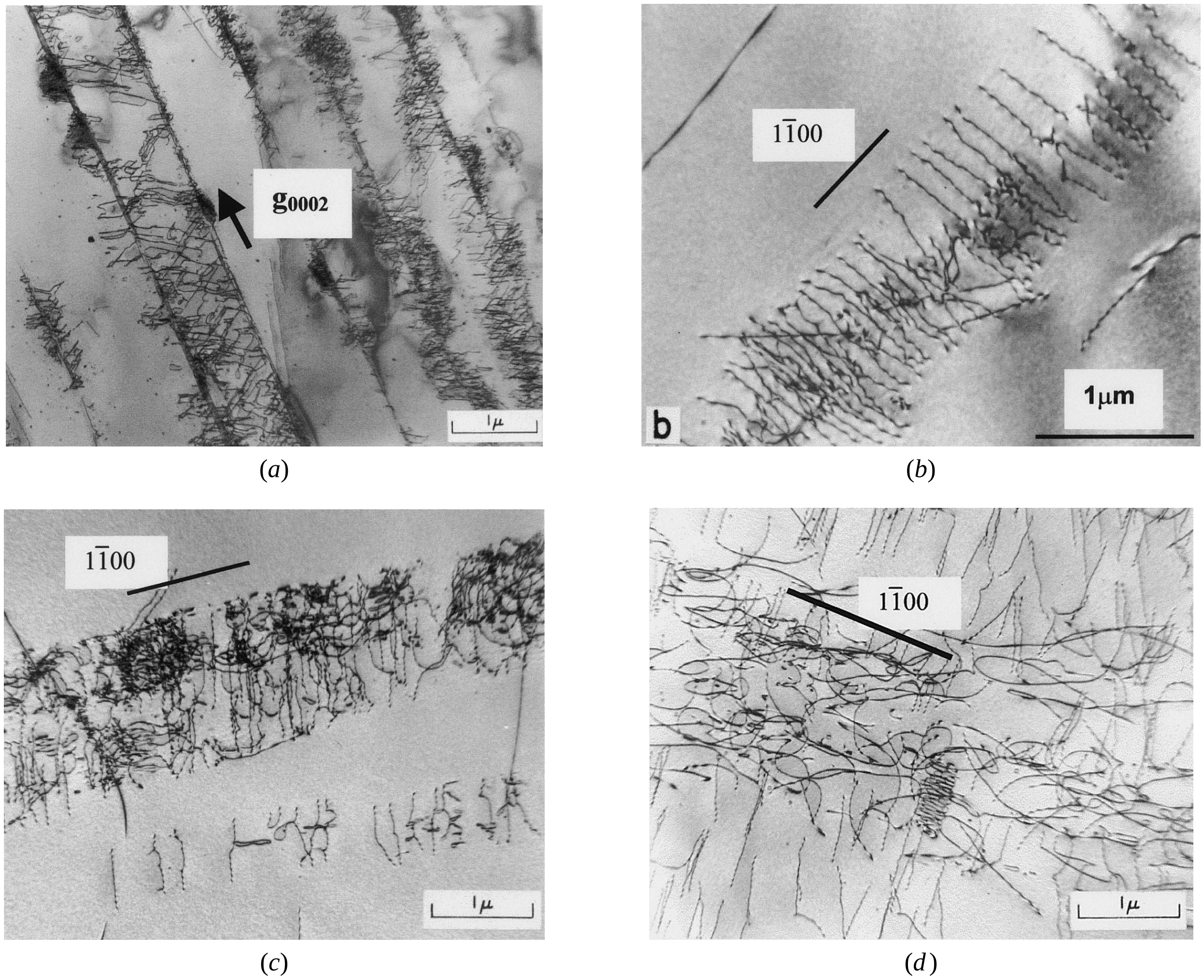

Fig. 15—Bright-field TEM micrographs showing changes in ⟨**a**⟩ dislocation arrangements as a function of temperature in Ti-5 pct Al crystals oriented for prism slip: (*a*) 77 K, (*b*) 300 K, (*c*) 600 K, and (*d*) 1000 K.

were loaded in the described orientation. The twin volume fraction is low, and the amount of strain accommodated by twinning continually decreases with increasing temperature. The observed twinning was all of the $\{10\bar{1}2\}$ type for the compositions studied, including the occasional deformation twins observed in Ti-5 wt pct Al crystals. This twin mode is a tension twin in α-titanium, *i.e.*, one that forms when tension is applied parallel to the *c*-axis. This twinning mode was identified using two-surface optical trace analysis as well as electron diffraction results from TEM. Operation of this mode is consistent with the loading applied in these tests, because compression normal to the *c*-axis is equivalent to tension parallel to it.

C. *Crystals Oriented for Nonbasal Deformation*

The Burgers vector for ⟨**c** + **a**⟩ slip is 1/3 $\langle 11\bar{2}3\rangle$. Possible slip planes that contain this vector are of the type $\{10\bar{1}0\}$, $\{10\bar{1}1\}$, and $\{11\bar{2}2\}$.[10,18] Analysis of the surface-deformation traces showed that the majority of crystals deformed in a complex manner, frequently incorporating more than one slip system as well as twinning. In order to maintain consistent comparisons, the critical shear stress was always resolved onto a $\{10\bar{1}1\}$ plane, although secondary slip on $\{11\bar{2}2\}$ planes was often observed.

The temperature dependence of the shear stress for ⟨**c** + **a**⟩ slip, resolved onto the $\{10\bar{1}1\}$ plane for the various aluminum-content crystals, is shown in Figure 18. The positive dependence of resolved shear stress on temperature is observed for the low-aluminum-content crystals and corresponds to situations where considerable shear strain is accommodated by twinning.[3,19] The dominant twin mode for Ti-1.4 pct Al compressed parallel to [0001] is $\{11\bar{2}2\}$, although a few twins of type $\{11\bar{2}4\}$ and $\{10\bar{1}2\}$ were observed at 77 and 190 K. The appearance of $\{10\bar{1}2\}$ twins is not expected in compression loading due to the sense of the twinning shear with respect to the applied stress; however, in the observed cases, the twins appear to emanate from the complex stress distribution around intersecting $\{11\bar{2}2\}$ twins and are, therefore, not a direct result of the applied load. There also is the possibility that the $\{10\bar{1}2\}$ twins could have occurred on unloading, but there is no simple way to confirm or dismiss this possibility. The effect of temperature on the twinning frequency in this alloy can be seen in Figure 19. There also is a transition in twinning behavior near 800 to 900 K, such that at 900 K, the twins are of the type $\{10\bar{1}1\}$. This is consistent with the results of Paton,[11,12] who showed that iodide titanium deformed in large part by deformation twinning on $\{10\bar{1}1\}$ at temperatures in excess of 700 K.

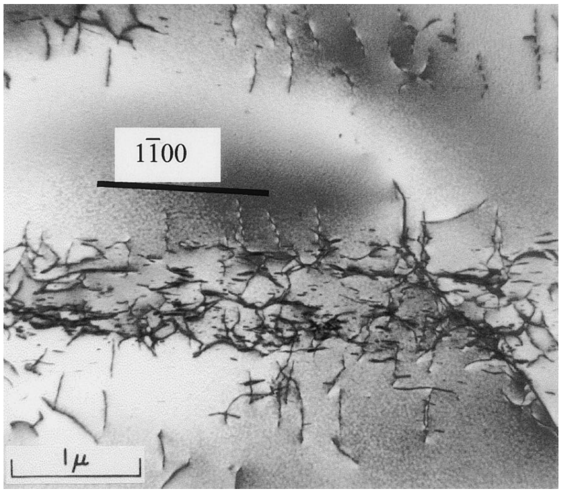

(*a*)

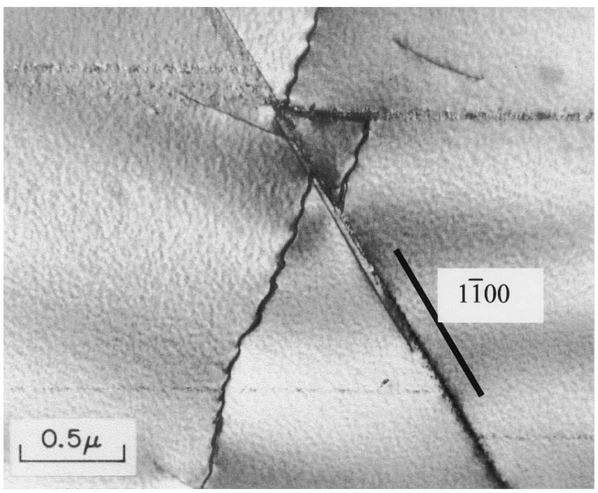

(*b*)

Fig. 16—Showing the effect of Al concentration on the arrangement of ⟨**a**⟩ dislocations during prism slip: (*a*) Ti-1.4 pct Al and (*b*) Ti-5 pct Al (note out of contrast horizontally oriented slip bands).

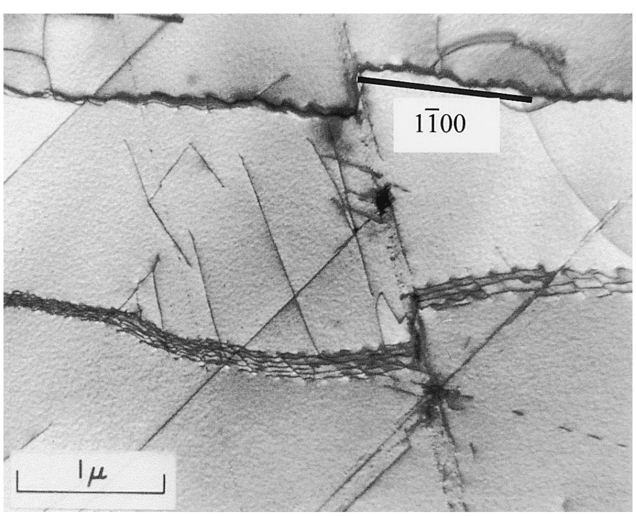

Fig. 17—Bright-field TEM micrograph showing shearing of sub-boundaries by ⟨**a**⟩ prism slip bands.

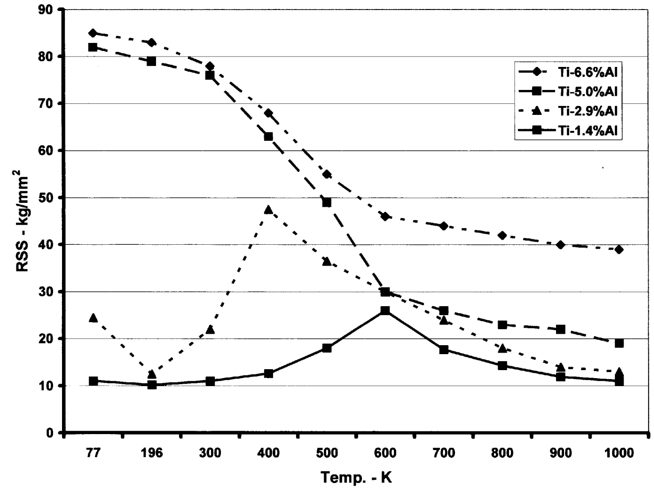

Fig. 18—Resolved shear stress as a function of temperature for different Al concentrations for single crystals loaded parallel to the *c*-axis.

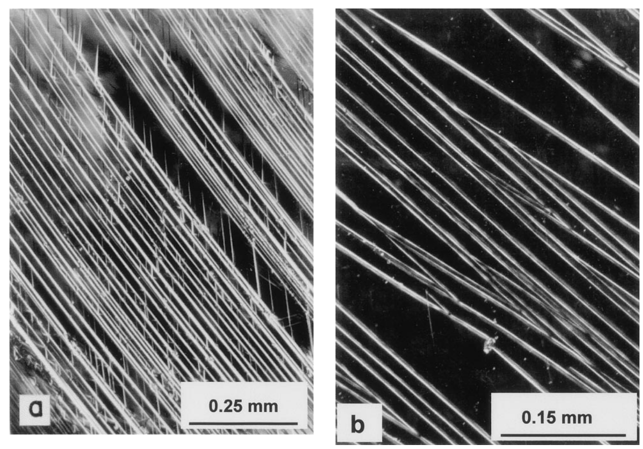

Fig. 19—Light micrographs showing the decrease in twin frequency with increasing deformation temperature in T-1 pct Al compressed parallel to [0001]: (*a*) 77 K and (*b*) 1000 K.

Type $\{10\underline{1}1\}$ twins are typically narrower than the other types of twins seen in α-Ti.

The Ti-2.9 pct Al crystals exhibited a distinct twin transition from $\{11\underline{2}4\}$ twins at 77 K to $\{11\underline{2}2\}$ twins at 400 K. Intermediate between these temperatures, a combination of the two twin types was observed. There was also considerably more slip activity in the higher-aluminum alloy crystals, and the twin width also decreased as the aluminum content increased. This transition in twin type is illustrated in Figure 20. The transition to $\{10\underline{1}1\}$ twinning also occurred with this alloy, and these twins were observed by two-surface trace analysis at both 900 and 1000 K.

Compared to the 1.4 and 2.9 pct Al crystals, the frequency of twinning rapidly decreased as the Al content increased to 5 or 6.6 pct. In fact, twinning is rarely observed during compressive deformation of the 5 and 6.6 pct Al crystals with a *c*-axis orientation. Consistent with the decreased extent of twinning, the temperature dependence of the shear stress for Ti-5 pct Al and Ti-6.6 pct Al also decreases monotonically from 77 K, instead of initially increasing with temperature, as seen in Figure 18. Trace analysis of surface slip planes showed that ⟨**c** + **a**⟩ slip primarily occurs on the $\{10\underline{1}1\}$

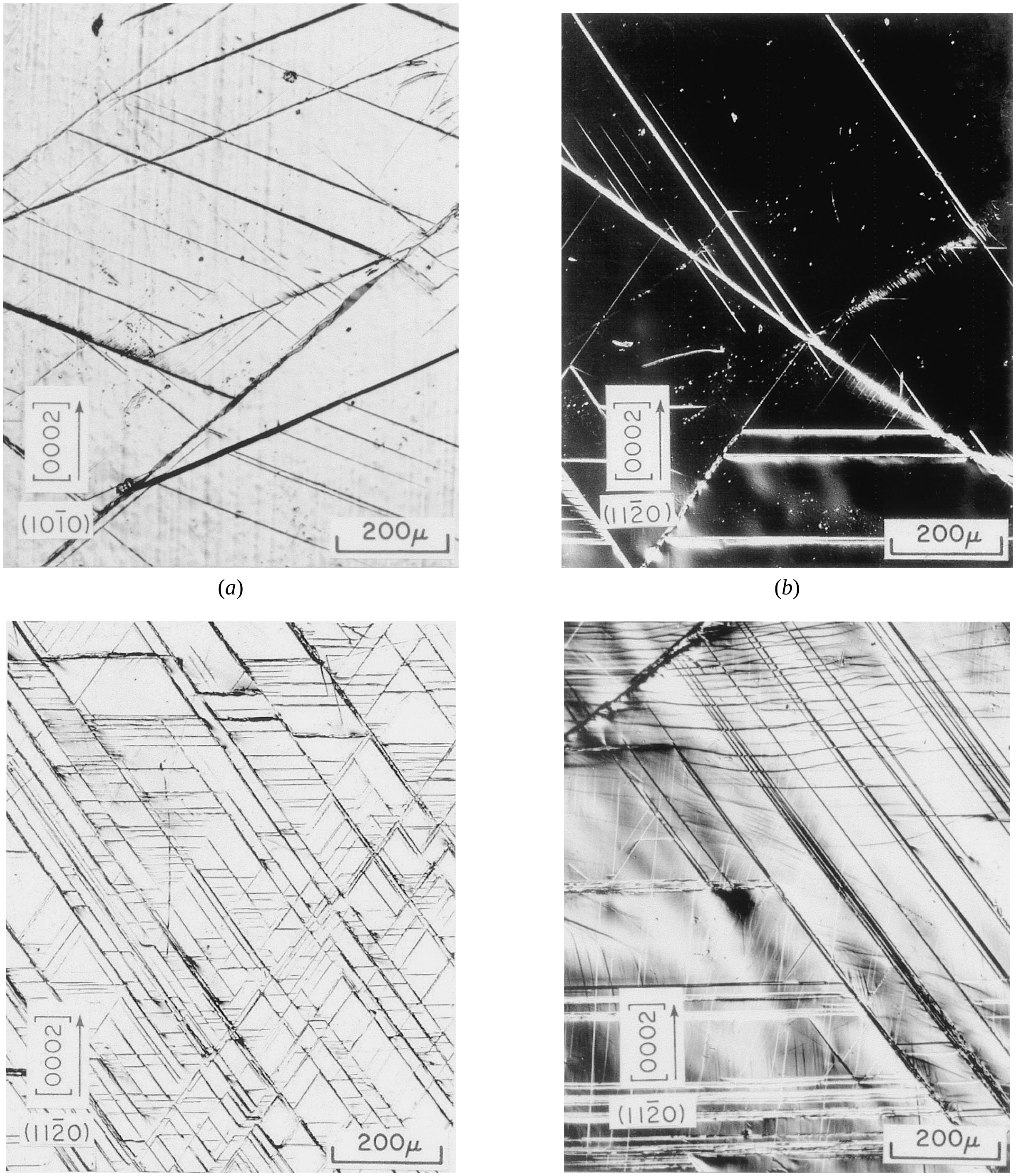

(*a*) (*b*)

(*c*) (*d*)

Fig. 20—Showing the transition in twin type and frequency with increasing deformation temperature in Ti-2.9 pct Al compressed parallel to [0001]: (*a*) 77 K, (*b*) 190 K, (*c*) 400 K, and (*d*) 500 K.

and {11$\bar{2}$2} planes. The ⟨**c** + **a**⟩ Burgers vector was identified using TEM, as shown in Figure 21. The slip tends to be very planar (Figure 22(a)) and the remaining dislocations, even at low temperatures, are mainly edge in character. This is in contrast to ⟨**a**⟩ slip, where mostly long, straight screw dislocations are seen. At elevated temperatures, substantial cross slip occurs, which makes slip-plane trace analysis difficult. Figure 22(b) also illustrates the difficulty encountered in assigning a low-index slip plane to the high-temperature slip traces.

An unexpected but important aspect of the deformation behavior in the higher-Al-content crystals, particularly the 5 and 6.6 pct Al alloys, is the occurrence of a catastrophic shear process. This process is one in which the crystal fails abruptly by shearing during compression testing. Although the macroscopic strain may be only a few percentages, a several-thousand-percent shear strain can be concentrated in a very narrow band of crystal. Increasing the aluminum content or increasing the deformation temperature caused a marked reduction in the ease of operation of ⟨**c** + **a**⟩ slip.

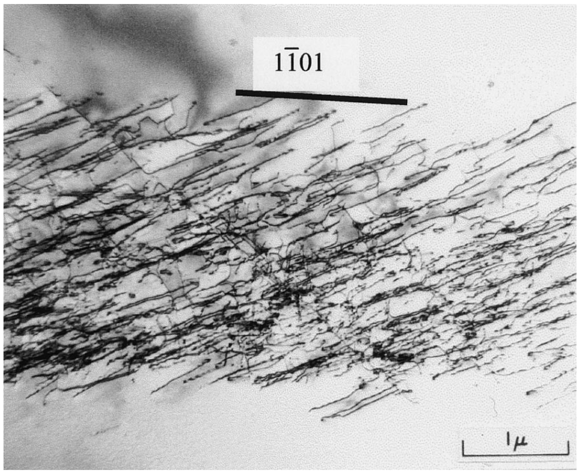

Fig. 21—Bright-field TEM micrograph taken with $\mathbf{g}_{0002}$ showing a slip band containing $\langle \mathbf{c} + \mathbf{a} \rangle$ dislocations.

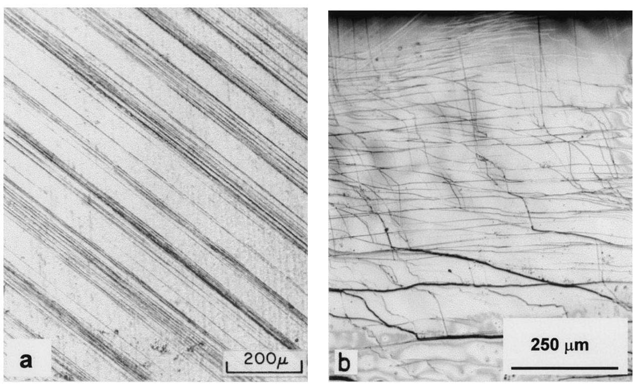

Fig. 22—Surface slip lines on crystals deformed parallel to the *c*-axis showing the effect of temperature and Al concentration on the amount of cross slip: (*a*) Ti-6.6 pct Al deformed at 300 K and (*b*) Ti-5 pct Al deformed at 900 K.

Fig. 23—An example of the unstable shear observed in Ti-5 and 6.6 pct Al crystals loaded parallel to [0001].

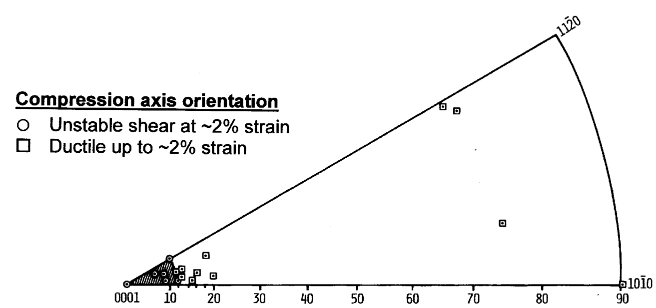

Fig. 24—Showing the behavior of misoriented crystals relative to occurrence of unstable shear.

Figure 23 illustrates the nature of this shear process. In this particular case, a cylindrical crystal was used to ensure that the corners of the usual rectangular specimens were not inducing the shear. The result shows that this is not the case. Attendant to the onset of this instability is the decrease and virtual disappearance of $\langle \mathbf{c} + \mathbf{a} \rangle$ slip with increasing temperature in both the 5 and 6.6 pct Al crystals. Such a reduction in $\langle \mathbf{c} + \mathbf{a} \rangle$ must result in the introduction of an alternate deformation process. This process results in an abrupt separation of the crystal along a planar band which accommodates the imposed strain. This occurrence has been termed "unstable shear." In Ti-5 pct Al, initiation of unstable shear occurred at 300 K and was observed to the highest test temperature (1000 K). With Ti-6.6 pct Al, unstable shear was observed at 190 K, and operation of this mode continued to 1000 K. The presence of α_2 phase in aged Ti-6.6 pct Al did not significantly influence this behavior. This shearing effect was not as pronounced in the Ti-2.9 pct Al crystals, although some specimens also exhibited this phenomenon to temperatures as high as 1000 K.

Since unstable shear may have important implications with regard to the forming of commercial alloys, an in-depth examination was made of this phenomenon. It has been observed that these same alloy crystals are ductile when undergoing prism or basal slip. Therefore, the possibility of an orientation dependence of unstable shear was investigated. Specimens of Ti-5 pct Al were prepared such that the basal-plane pole of the nominally *c*-axis crystals had an increasing misorientation from the loading axis, as described earlier in Figure 1(d). The compression axis for each crystal tested is shown in Figure 24, and the type of symbol shows whether that crystal sheared unstably or was ductile up to several percentages of strain. From Figure 24, it can be seen that there is an abrupt change in propensity for unstable shear with change in the loading-axis orientation. Those crystals whose axes were ~12 deg (or greater) from [0001] sustained a larger strain prior to the onset of unstable shear in comparison to crystals whose loading axes were aligned more closely to the [0001] direction. In an attempt to elucidate the source of these differences in behavior, thin foils were prepared from specimens whose orientations were 7 deg (sheared crystal) and 20 deg (ductile crystal) from the (0001) axis. The TEM examination showed a preponderance of $\langle \mathbf{c} + \mathbf{a} \rangle$ dislocations in both specimens.

To investigate the details of the early stage of unstable

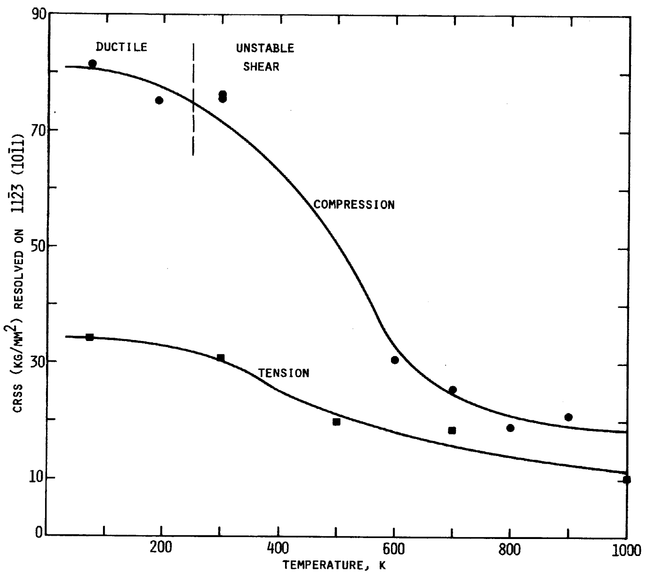

Fig. 25—Resolved shear stress in *c*-axis oriented crystals loaded in tension and compression.

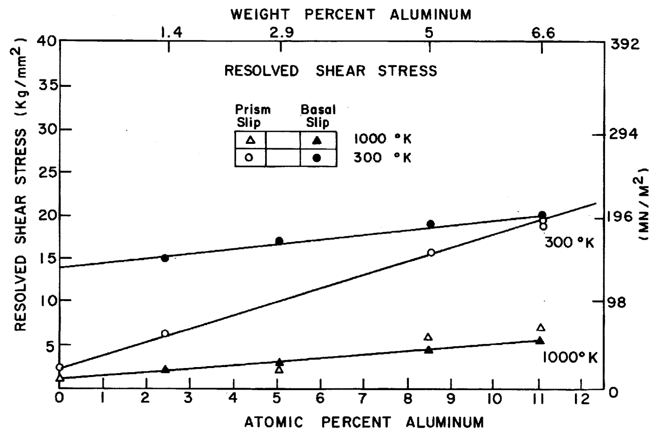

Fig. 26—Resolved shear stress for prism and basal slip as a function of Al concentration for crystals deformed at 300 K and 1000 K.

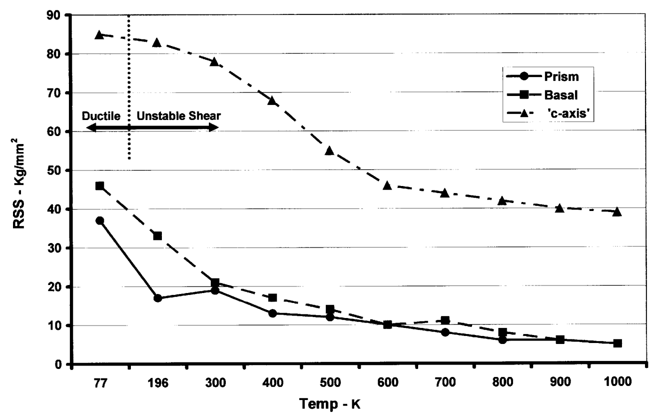

Fig. 27—RSS vs deformation temperature for prism, basal, and *c*-axis deformation in Ti-6.6 pct Al single crystals.

shear, Ti-5 pct Al crystals have also been tested using repeated loading experiments with successively higher loads. Examination of the prepolished surfaces has revealed significant deformation occurring on several $\langle \mathbf{c} + \mathbf{a} \rangle$ slip systems prior to fracture. The fractures produced by the shear process were quite straight and planar. The traces of the fracture planes have been identified as $\{10\bar{1}2\}$, $\{11\bar{2}2\}$, $\{11\bar{2}3\}$, and $\{11\bar{2}4\}$. These also are common twinning planes in α-Ti, but the fractures could not definitely be associated with the occurrence of twinning. Thin foils prepared from sections adjacent and parallel to a $\{10\bar{1}2\}$ fracture plane in a Ti-5 pct Al crystal contained very wide twins with an extremely high dislocation density present within the twin. The effect of varying the strain rate was examined to see if a slower strain rate would permit the crystal to deform without shearing. The strain rate was reduced by a factor of 2, and no change was observed in unstable shear behavior.

The results up to this point were obtained with a compressive loading axis normal to the basal planes. Single crystals of Ti-5 pct Al were also tested in tension by preparing specimens using diffusion-bonding techniques described in Section II. The resolved shear stress for tension and compression loading was determined as a function of temperature, and these results are plotted in Figure 25. The difference in yield stress is quite marked for the two loading methods, and the reason appears to be related to a tension-compression asymmetry in deformation mode. The tension-loaded crystals exhibited extensive $\{10\bar{1}2\}$ twinning, whereas the compression-loaded crystals deformed by $\langle \mathbf{c} + \mathbf{a} \rangle$ slip up to the strain corresponding to the onset of unstable shear. This result is somewhat surprising, in view of the suppressed twinning in this alloy under compressive loading conditions. Also, the tension-loaded crystals were very ductile and did not exhibit unstable shear.

II. DISCUSSION

A. *Deformation Behavior*

The present results show that both Al and deformation temperature have a pronounced effect on both the resolved stress for slip in Ti-Al alloys and on the deformation character. Most significantly, the relative changes in CRSS with Al concentration are such that basal slip should become increasingly important with increasing Al concentration. This is shown in Figure 26, in which the data for prism and basal slip have been plotted against Al concentration for tests conducted at 300 and 1000 K. Examination of these data show that solution hardening occurs for both prism slip and basal slip at both temperatures, but that hardening is much more rapid for prism slip than for basal slip at 300 K. This suggests that prism slip would be expected to dominate polycrystal deformation in dilute alloys at 300 K; prism and basal slip should be about equally important in deformation of Ti-Al alloys when the Al concentration reaches 5 to 6 pct Al. Further, for deformation at 1000 K, both prism and basal slip would appear to be equally favored over the entire range of alloy compositions. The relative importance of prism and basal slip at other temperatures can be seen by comparing the data in Figures 2, 14, and 18, although this comparison is complicated by the intervention of twinning in the crystals oriented for basal slip. This intervening deformation mode results in a nonlinear temperature dependence of CRSS on temperature, as shown in Figures 2 and 18.

An estimate of the propensity for $\langle \mathbf{c} + \mathbf{a} \rangle$ slip, in comparison to that for prism and basal slip, can be made from the data in Figure 27. From this figure, it can be seen that the resolved shear stress for $\langle \mathbf{c} + \mathbf{a} \rangle$ slip is consistently higher than that for $\langle \mathbf{a} \rangle$ slip on prism or basal planes. Using these data for the Ti-6.6 pct Al crystals, it can be seen that the resolved shear-stress ratios for $\langle \mathbf{c} + \mathbf{a} \rangle$ and $\langle \mathbf{a} \rangle$ slip on either the prism or basal planes is consistently higher. These ratios vary from about a factor of 2 at 77 K to approximately 7 or 8 at 1000 K. Consequently, $\langle \mathbf{c} + \mathbf{a} \rangle$ slip is always more difficult to activate than either prism or basal slip, and this is also true for pure Ti, as pointed out by Paton and Backofen.[3,19] However, $\langle \mathbf{c} + \mathbf{a} \rangle$ slip occurs during deformation of polycrystalline Ti alloys. It is an important deformation mode, because it has much to do with the ductility of commercial high-strength Ti alloys. These alloys always have sufficiently high Al concentrations and small enough grain sizes that deformation by twinning seldom occurs.

The influence of α_2 precipitation on CRSS for prism slip in the aged Ti 6.6 pct Al crystals was found to be negligible. This was somewhat surprising, because the size and density of precipitates was such that considerable precipitation hardening might have been expected.[12,13] The explanation for this apparently lies in the fact that the precipitates are coherent, with a very small misfit, as evidenced by the total absence of coherency-strain contrast in bright-field images of the precipitates. In addition, there is a relatively small difference in modulus between the α and α_2 phases, thus giving rise to weak interactions with moving dislocations. The only noticeable effect of the α_2 precipitates was to promote highly planar slip, evidently as the result of the shearing of the coherent, ordered precipitates. This change in slip character is probably responsible for the reduced ductility, which is often encountered in alloys containing a significant volume fraction of α_2, rather than an increased strength, as might be expected. Commercial alloys containing Al and Sn concentrations totaling approximately 6 wt pct show precipitation hardening due to α_2 formation. This suggests that the difference in strengthening behavior between polycrystals and single crystals is related to a change in the boundary-hardening contribution to the overall strength of the alloy.

Slip character is one of the aspects of deformation behavior most affected by Al additions to Ti. The effect is illustrated by comparing, for example, Figures 9 and 13. Figure 13(b) shows the typical dislocation arrangements characteristic of the wavy slip which occurs in Ti-1.4 pct Al at 300 K. Figure 9 shows the typical dislocation arrangements in a Ti-5 pct Al crystal deformed at the same temperature but exhibiting planar slip, such as that shown in Figure 8(b). A similar transition from planar to wavy slip occurs with increasing temperatures in the higher-Al-content alloys, as is shown in Figure 10 for basal slip and in Figure 15 for prism slip. The tendency toward planar slip either in the higher-Al-content alloys or at lower deformation temperatures is probably a consequence of the presence of short-range order,[13] which has been reported to restrict the operation of cross slip.

Many of the reported observations concerning changes in deformation behavior and the formation of preferred orientation (texture) in polycrystals can be rationalized in terms of the data presented here. Of particular importance is the increased tendency toward basal slip with increasing Al concentration and the operation of $\langle \mathbf{c} + \mathbf{a} \rangle$ slip. Both of these factors must be accounted for when calculating or even explaining the occurrence of texture in commercially produced Ti alloys.

B. *Unstable Shear*

When unstable shear occurs, the crystal undergoes gross localized deformation in a very narrow shear band. There are two plausible mechanisms that may account for this gross deformation in the shear band, and they both require a sudden reorientation of the lattice. Once the lattice has been locally reoriented, the Schmid factor for $\langle \mathbf{a} \rangle$ slip increases (it was initially zero), and the stress level is sufficient to cause significant deformation in the zone. This may be in the form of either prism or basal slip, depending on the details of the reorientation, since both systems have similar CRSS values for slip. Reorientation can result from either twinning or dislocation interactions to form kink bands. Once lattice reorientation occurs, gross slip results, with an attendant rise in temperature due to adiabatic heating within the band. Adiabatic heating is particularly important in Ti alloys because of their low thermal diffusivity. This temperature increase further reduces the CRSS and produces an unstable shear situation. A similar, possibly related reaction occurs in Be single crystals when loaded in compression parallel to the *c*-axis.[20] Planar shear failures are observed in Be, which coincide with $\{11\underline{2}4\}$ and $\{10\underline{1}2\}$ planes in a similar way to the shear planes in Ti reported herein. In addition, Damiano, *et al.*[20] also observed premature failure initiated by a kinking mechanism incorporating basal slip when a subgrain structure was present in the crystal. A misorientation of one-half of a degree with respect to the load axis was sufficient to nucleate a kink band. Some $\{10\underline{1}2\}$ twins were observed, which had also undergone extensive slip inside the twins. This was interpreted to indicate that, once the twin formed, the Be crystal was able to undergo deformation within the reoriented region of the twin. Similar evidence obtained in this work for α-Ti-Al tends to support the idea that local reorientation occurs by either kink-band formation or twin formation. One example of a highly localized reorientation of the lattice is shown in Figure 6. Unique slip traces are seen inside the deformation band, as well as a set of slip lines which deviates from the bulk lattice on crossing into the band. When the trace analysis is compared to the common Ti twinning planes, only the $\{11\underline{2}1\}$ twinning plane would fit. It is unlikely that this band is a $\{11\underline{2}1\}$ twin, since the shear strain is opposite to the strain resulting from compressive loading.

The bands which represent reorientation of the crystal are sharply defined and are crystallographically distinct. That is, X-ray Laue patterns taken from these regions show distinct and sharp splitting of the diffraction spots. If the crystal had deformed more homogeneously, severe asterism in the diffraction spots would have resulted.

The propagation of shear cracks along these reoriented regions appears quite striking, and evidence to suggest both twins and kink bands has been observed in this study. For example, a crack was been observed to start propagating along a $\{11\underline{2}3\}$ path in a region which resembles a kink band. No evidence of twin formation was seen. During subsequent reloading, the crack had extended further and changed direction, corresponding to a $\{11\underline{2}4\}$ plane. Finally, the crack was observed to be moving along a region of severe lattice distortion, not parallel to the observed slip traces. Highly distorted bands without associated cracks also were observed in the vicinity of slip bands. Regions adjacent to fractures, which appear to be twins, also have been seen.

When the crystal is purposely oriented off the *c*-axis by approximately 12 deg, large amounts of slip are able to occur. In this case, several slip systems are activated and the crystal is ductile. Figure 24 showed the orientation dependence of unstable shear in crystals misoriented from [0001]. In these cases, deformation bands are developed, in which both $\langle \mathbf{c} + \mathbf{a} \rangle$ and $\langle \mathbf{a} \rangle$ slip systems are operating.

There is a well-known phenomenon observed in the processing of commercial, high-strength Ti alloys called strain-induced porosity (SIP). When SIP occurs, it results in small voids in the material. These voids, if undetected, can serve as fatigue-crack initiation sites. Therefore, the current observations of unstable shear provide some insight into the occurrence of SIP. The strong orientation dependence of unstable shear may also provide some possibilities to avoid SIP formation.

ACKNOWLEDGMENTS

This work was performed sometime ago when the authors were together working at the Rockwell Science Center. The work was supported by The Air Force Office of Scientific Research under Contract No. F44620-72-C-0043. Dr. Alan H. Rosenstein was the Contract Monitor. We are grateful to him for his encouragement, support, and patience. We also acknowledge the assistance of our technical support staff at Rockwell, especially H. Nadler, F. Nevarez, P. Sauers, and R. Spurling. We also thank Jon Blank, OSU, for assistance with completion of some of the references.

REFERENCES

1. D. Lee and W.A. Backofen: *Trans. AIME*, 1966, vol. 236, pp. 1696-1704.
2. D.N. Fager and W.F. Spurr: *Trans. ASM*, 1968, vol. 61, pp. 283-92.
3. N.E. Paton and W.A. Backofen: *Metall. Trans.*, 1970, vol. 1, pp. 2839-47.
4. E.D. Levine: *TMS-AIME*, 1966, vol. 236, pp. 1558-65.
5. K.R. Evans: *TMS-AIME*, 1968, vol. 242, pp. 648-53.
6. R.N. Orava *et al.*: *Trans. ASM*, 1966, vol. 59, pp. 171-84.
7. T.R. Cass: in *The Science, Technology and Application of Titanium*. R.I. Jaffee and N.E. Promisel, eds., Pergamon Press, London, 1970, pp. 733-39.
8. T. Sakai and M.E. Fine: *Acta. Met.*, 1974, vol. 22, pp. 1359-72.
9. P.G. Partridge: *Met. Rev.*, 1967, vol. 12, pp. 169-94.
10. H.S. Rosenbaum: in *Deformation Twinning*, R.E. Reed-Hill, J.P. Hirth, and H.C. Rogers, eds., Gordon and Breach Science Publishers, New York, NY, 1964, pp. 43-76.
11. J.C. Williams and M.J. Blackburn: *Phys. Status Solidi*, 1968, vol. 25, pp. K1-K3.
12. D.R. Thornburg and H.R. Piehler: *Titanium Sci. Technol.*, 1973, vol. II, pp. 1187-97.
13. M.J. Blackburn and J.C. Williams: *ASM Q. Trans.*, 1969, vol. 62, pp. 398-409.
14. J.C. Williams and G. Luetjering: in *Titanium '80, Science and Technology*, H. Kimura and O. Izumi, eds., TMS-AIME, Warrendale, PA, 1981, vol. 1, pp. 671-81.
15. M.J. Blackburn and J.C. Williams: *Trans. AIME*, 1967, vol. 239, pp. 287-88.
16. J.C. Williams: The Boeing Company, Seattle, WA, unpublished research, 1966.
17. W.H. Hartt and R.E. Reed-Hill: *Trans. AIME*, 1967, vol. 239, pp. 1511-14.
18. E. Tenckhoff: *Z. Metallkd.*, 1972, vol. 63, pp. 192-97.
19. N.E. Paton and W.A. Backofen: *Trans. TMS-AIME*, 1969, vol. 245, pp. 1369-70.
20. V.V. Damiano, J.E. Hanafee, G.J. London, and N. Inoue: *Trans. TMS-AIME*, 1969, vol. 245, pp. 637-49.